Tracking of myelin-reactive T cells in EAE animals using small particles of iron oxide and MRI.

Non Peer-reviewed author version

BAETEN, Kurt; ADRIAENSENS, Peter; HENDRIKS, Jerome; THEUNISSEN, Evi; LAMBRICHTS, Ivo; GELAN, Jan; HELLINGS, Niels & STINISSEN, Piet (2010)
Tracking of myelin-reactive T cells in EAE animals using small particles of iron oxide and MRI.. In: NMR IN BIOMEDICINE, 23(6). p. 601-609.

DOI: 10.1002/nbm.1501
Handle: http://hdl.handle.net/1942/10712

Tracking of myelin-reactive T cells in EAE animals using small particles of iron oxide and MRI

Baeten Kurt[1], Adriaensens Peter[2], Hendriks Jerome[1], Theunissen Evi[1], Ivo Lambrichts[1], Gelan Jan[2], Hellings Niels[1] and Stinissen Piet[1]

Hasselt University, [(1)]Biomedical Research Institute [(2)]Institute of Material Research (IMO)-chemistry division, and School of Life Sciences, Transnational University Limburg, B-3590 Diepenbeek, Belgium

Corresponding author:
Prof. Dr. Piet Stinissen
Hasselt University Dept. Biomed
Agoralaan – Building C
3590 Diepenbeek
Belgium
Tel: +32 11 26 92 04
Fax: +32 11 26 92 09

e-mail: piet.stinissen@uhasselt.be

Abstract

Myelin-reactive T cells are responsible for initiating the cascade of autoreactive immune responses leading to the development of multiple sclerosis. For better insights into the disease mechanism, it is of major importance to have knowledge on the sites at which these cells are active during disease progression. Hereto, we investigated whether it is possible to track myelin reactive T cells, upon labelling with SPIO particles, in the CNS of EAE animals by MRI. First, we determined the optimal labelling condition leading to a high particle uptake and minimal SPIO-PLL aggregate formation using Prussian blue stainings and inductively coupled plasma spectroscopy measurements. Results from labelling of rat derived myelin reactive T cells with low concentrations of SPIO particles (i.e. 25 µg/ml) in combination with different concentrations of PLL (0 – 1.5 µg/ml) showed that increasing amounts of PLL led to augmented levels of free remnant SPIO-PLL aggregates. In contrast, a low PLL concentration (i.e. 0.5 µg/ml) combined with high concentrations of SPIO (i.e. 400 µg Fe/ml) led to a high labelling efficiency with minimal amounts of aggregates. Second, the labelled myelin-reactive T cells were transferred to control rats to induce EAE. At the occurrence of hindlimb paralysis, the SPIO labelled myelin reactive T cells were detected in the sacral part of the spinal cord and shown to be highly confined to this region. However, upon transfer in already primed rats, transferred T cells were more widely distributed in the CNS and shown present in the spinal cord as well as in the brain. Our study demonstrates the feasibility to track SPIO labelled myelin-reactive T cells in the spinal cord as well as the brain of EAE rats upon systemic administration. Furthermore, we provide data on the optimal labelling conditions for T cells leading to a high particle uptake and minimal aggregate formation.

Key words: Experimental autoimmune encephalomyelitis, SPIO, MRI, T cell, multiple sclerosis

Graphical Abstract

Tracking of myelin-reactive T cells in EAE animals using small particles of iron oxide and MRI

Kurt Baeten, Peter Adriaensens, Jerome Hendriks, Evi Theunissen, Ivo Lambrichts, Jan Gelan, Niels Hellings and Piet Stinissen*

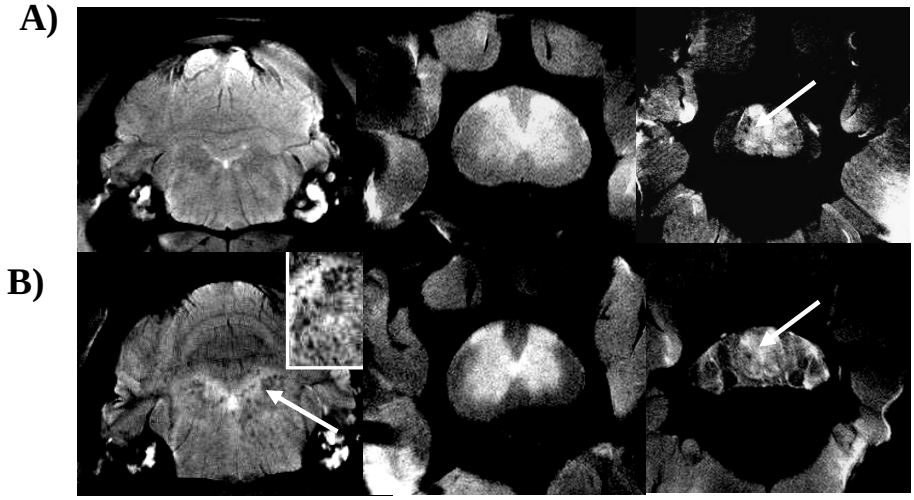

We demonstrate the feasibility to track SPIO labelled myelin reactive T cells in the spinal cord as well as the brain of recipient rats upon systemic administration. Data are provided on an optimal labelling protocol towards a high particle uptake by rat T cells, minimal aggregate formation and without any effect on the viability and functioning of the cells. When applying this method to understand the role of autoreactive T cells in the disease initiation and progression of experimental autoimmune encephalomyelitis (EAE), we revealed different infiltration patterns of myelin-reactive T cells in naive rats (A) and actively immunised EAE rats (B).

Introduction

One of the primary mechanisms thought to be involved in multiple sclerosis (MS) is the peripheral activation of myelin reactive T cells, which initiates an immune cascade leading to the destruction of myelin and the induction of death of neurons and oligodendrocytes (1-3). The important role of myelin-reactive T cells in the development of MS was shown by the induction of experimental autoimmune encephalomyelitis (EAE) after transfer of myelin reactive T cells in a susceptible animal (4). In the subsequent years several attempts were made to track these cells in the recipient animals to get a better understanding of the role of these cells in the disease process. Bioluminescent imaging (BLI) is able to provide us with a general view on the distribution of the transferred cells but lacks in depth view and also quantification is rather difficult. BLI experiments in primed EAE mice showed an initial allocation of the transferred myelin-reactive T cells to the peripheral immune organs followed by a migration to the CNS at day three post transfer (5). However, in naive mice the myelin-reactive T cells induced EAE but no CNS infiltration of the transferred cells could be detected by BLI. In another approach myelin reactive T cells were retrovirally transfected with green fluorescent protein (GFP) (6). Flow cytometric analysis at different time points post transfer of the homogenised central nervous system (CNS) and immune organs of animals led to quantitative data on the migration pattern of the pathogenic T cells. However, this method does not give insights into the spatial distribution and migration of the myelin reactive T cells within the CNS itself nor is it possible to perform an in vivo follow up. Intravital microscopy could overcome some

of these obstacles though the in depth view and the area that can be visualised is seriously restricted.

With the development of paramagnetic small particles of iron oxide, MRI has become an interesting tool to perform cell tracking studies. This technique offers the unique combination of cell tracking throughout an entire organism/animal and highly detailed anatomical information on the surrounding tissue. In recent years, several studies were conducted investigating the feasibility of tracking immune cells and stem cells using these paramagnetic particles (7-16). Regarding the tracking of T cells, two different approaches were developed. Pirko et al. demonstrated that injection of anti-CD4 antibodies linked to paramagnetic particles in mice with encephalomyelitis could lead to the detection of CD4+ T cells in the CNS during inflammation (17). However, this method does not allow a specific follow up of a transferred cell population since no discrimination can be made between transferred and host cells. Hereto, a second approach was developed in which cells were in vitro labelled with paramagnetic particles and transferred in the host of interest. Several studies showed the feasibility of in vitro labelling of monocyte-derived cells with paramagnetic iron oxide particles (SPIO) (18-20). However, it became clear that labelling of poorly phagocyting cells, like T cells, requires the use of a transfection agent or signalling peptides like the HIV-tat peptide (21-24). These agents were indicated to significantly increase the labelling efficiency by the formation of a positive charged surface. Recently however, Montet-Abou and co-workers indicated that the addition of positively charged transfection agents (TAs) can lead to particle aggregation and demonstrated the necessity of a careful re-examination of the amount and ratios of iron oxide particles and transfection agent to be used (25). After all Fe-TA complexes, present in the injected cell

suspension, can be taken up by monocyte derived cells and cause aspecific hypo intense areas upon infiltration of these cells in the CNS.

In the present study we investigated whether it is possible to track myelin reactive T cells with MRI in the spinal cord as well as the brain of rats upon systemic administration. To this end we determined the optimal labelling conditions for activated rat myelin reactive T cells using SPIO particles in combination with the transfection agent poly-L-lysine (PLL) in order to achieve a maximal labelling efficiency and a minimal amount of particle aggregation.

Experimental

Generation of myelin reactive T cells

All animal experiments were approved by the local Ethical Committee for Animal Experiments of Hasselt University, Diepenbeek, Belgium. Female Lewis rats (Harlan CPB, Zeist, The Netherlands) were subcutaneously injected with a 0.1 ml suspension containing 250 µg/ml myelin basic protein (MBP), 2.5 mg/ml H37RA heat-killed mycobacterium tuberculosis and 60 µl Complete Freund's adjuvant in both hind paws. Inguinal and popliteal lymph nodes were isolated at day 9 post immunization (p.i.). A cell suspension was obtained by passing the tissue through a steel mesh. Cells were washed and resuspended in medium (RPMI 1640 supplemented with penicillin/streptomycin, 20 µM 2-mercapto-ethanol, sodium pyruvate, non-essential amino acids) to which 1% rat serum and 33 µg/ml MBP was added. After three days cells were washed and resuspended in medium supplemented with 10% foetal calf serum (FCS) and 6,5% supernatans of Concanavaline stimulated spleen cells (CAS). At day ten after lymph node isolation, cells were restimulated using irradiated thymic cells. Subsequently, cells were incubated for 24hrs with IL-2 (6,5 v/v%), IL-12 (20 ng/ml; R&D Systems) and IL-18 (25 ng/ml; R&D Systems) and labelled with SPIO particles.

SPIO labelling

SPIO-PLL complexes were made by mixing different amounts of SPIO particles (Endorem; Guerbet, France) and PLL (MW > 300.000; Sigma-Aldrich, Belgium) in RPMI medium on a rotator for 30 minutes. The final concentrations of PLL and iron were varied between 0 to 1.5 µg/ml and 25 to 400 µg/ml respectively. Myelin reactive

T cells were adjusted to a volume of 4.10^6 cells/ml and an equal volume of SPIO-PLL solution was added. Cells were incubated for 24hrs and washed 3 times with phosphate buffered saline.

Histology and immunohistochemistry

To detect the presence of iron oxide particles in the labelled cell cultures, cells were fixed on PLL coated slides using 4% paraformaldehyde. Subsequently, cells were immersed for 60 minutes in Perls' solution containing 5% HCl and 5% potassium ferrocyanide. Counterstaining was performed using a Nuclear fast red solution (Klinipath, Belgium).

Immediately after MRI, brains and spinal cords were dissected, fixed with 4% paraformaldehyde and embedded in paraffin. Slices with a thickness of 10 µm were used for detection of iron contents and T cell infiltrates. The presence of iron was detected with a Prussian blue staining followed by a nuclear fast red counterstain as described earlier. For immunohistochemistry, an anti-CD3 antibody was used to detect T cell infiltrates (Serotec, UK). Binding of primary antibody was revealed by avidin-biotin-peroxidase with reagents supplied by Vector laboratories as previously described (Lawson 1990). Images were taken using a Nikon eclipse 80i microscope (Nikon).

Determination of iron concentration

The iron concentration of cells, labelled with different amounts of SPIO and PLL, was quantified by inductively coupled plasma spectrometry using a Perkin Elmer Optima. After labelling, cells were washed three times and lysates were obtained by dissolving pellets of 1.10^6 cells in 100 µl of an aqueous solution containing 65% HNO_3

and 10% H_2O_2. After one hour the suspension was further diluted to 1ml with H_2O. For Fe-measurements, the spectrometer was set to 239.56 nm and calibrated with 9 standards dissolved in HNO_3.

Estimating the percentage of labelled cells

The fraction of the cells containing iron oxide particles was examined by exploiting the magnetic properties of these particles. After labelling, cells were washed three times, dissolved in PBS and counted. The FACS tube containing the cell suspension was placed for 6 min in the Easysep Magnet (StemCell Technologies, France), gently inverted to discard the unbound cells, removed from the magnet and reconstituted with PBS. This process was repeated once to remove aspecifically bound cells.

Cell viability and functioning of labelled cells

To determine the effect of SPIO-PLL labelling on the functioning and the viability of myelin reactive T cells, the assays described below, were conducted directly after labelling and after a post labelling period of 72hrs in medium supplemented with 10% FCS and 6,5% CAS.

The microculture tetrazolium (MTT) assay was conducted on unlabelled and labelled T cells (400 µg Fe/ml, 1 µg PLL/ml) to examine the effect of labelling on cell viability. Briefly, cells were incubated with MTT solution for 4hrs at 37 °C after which the supernatant was removed and glycine, dissolved in dimethyl sulfoxide (DMSO), was added. The light absorbance was read at 540 nm. The activation status of the cells was examined by incubating the cells with anti-CD3 (PE; W3/25) (BD Biosciences,

Erembodegem, Belgium). and anti-CD25 (FITC; OX-39) (Immunotools, Friesoythe, Germany) antibodies. Flow cytometric measurements were performed on a FACS Calibur system (BD Biosciences) and analysed using CellQuest Software (BD Biosciences). The cytokine production was analysed after a 4hrs stimulation with phorbol myristate acetate (PMA) and calcium ionomycin (CaI). Subsequently, cells were incubated with anti-TCR (PercP; R73), anti-IFNγ (PE; DB-1) and anti-IL4 (PE; OX-81) (BD Biosciences, Erembodegem, Belgium) antibodies.

Transfer of labelled cells and induction of EAE

Labelled cells (7.10^7 cells) were adoptively transferred in naive rats (n=2) or injected at the onset of disease (i.e. day 10 p.i.) in actively immunised animals (n=2). The active immunisation was performed as described above for the generation of myelin reactive T cells. Rats were weighted and scored daily according to the following neurological scale: 0 = no neurological abnormalities, 0.5 = partial loss of tail tonus, 1 = complete loss of tail tonus, 2 = hind limb paresis, 3 = hind limb paralysis, 4 = moribund, 5 = death.

MRI experiments

Three to four days after transfer of labelled cells, rats were euthanized by decapitation. Post mortem MR imaging was performed in a 25 mm birdcage coil on a Varian Inova 400 spectrometer (Varian, Nuclear Magnetic Resonance Instruments, Palo Alto, California, USA), operating at 9.4 Tesla by using the multislice spin-warp technique (30). T2-weighed images were acquired with a repetition time (TR) of 2500 ms and an echo time (TE) of 65 ms and 18ms for respectively the brain and the spinal

cord. Coronal images of the brain had a slice thickness of 1.1 mm and an inplane resolution of 62.5 × 62.5 μm (FOV 25 mm × 25 mm) with gradient strengths of 4.69, 3.91 and 8.18 G/cm in the read, phase and slice direction. For the spinal cord, coronal images were acquired with a slice thickness of 1 mm and an inplane resolution of 43.3 × 43.3 μm (FOV 13 mm × 13 mm) with gradient strengths of 5.41, 4.52 and 7.42 G/cm in the read, phase and slice direction. All images were acquired with 12 averages leading to a total acquisition time for the entire CNS of approximately 11hrs.

Results

Labelling of activated T cells with SPIO-PLL complexes

In order to gain insights into the role of different T cell subsets in multiple sclerosis, it is of importance to be able to track these cells in different animal models during disease progression. To determine the optimal labelling condition leading to a high iron load and minimal particle aggregation, activated myelin reactive T cells were incubated with variable amounts of SPIO particles and PLL. Since it was previously shown that PLL is toxic at a concentration ≥ 2 µg/ml, the concentration was varied between 0 µg/ml and 1,5 µg/ml and combined with a fixed iron concentration of 25 µg/ml. This iron concentration was earlier shown useful in a study by Anderson et al. (7). After 24hrs cells were washed three times and a Prussian blue staining was performed to determine the cellular uptake of the SPIO particles as well as to detect SPIO-PLL complex aggregation. Figure 1A shows that incubating activated rat T cells with 25 µg Fe/ml without PLL results in a very low particle uptake. Adding increasing amounts of PLL augments the iron uptake by the cells, though only moderately. Furthermore, at increasing PLL concentrations augmented amounts of SPIO-PLL aggregates are present. The size and number of these complexes seem to correlate with the amount of PLL added. To improve the labelling efficiency, the concentration of SPIO particles added to the cell suspension was increased at a fixed PLL concentration of 1 µg/ml. The Prussian blue stainings show a serious increase in the amount of labelled cells at an iron concentration of 400 µg/ml. In addition, the free SPIO-PLL aggregates present when cells were incubated with a low Fe to PLL ratio, were almost completely absent.

Inductively coupled plasma mass spectroscopy (ICP) was performed in order to quantify the SPIO uptake by T cells in the different labelling conditions. Figure 1B demonstrates that incubating activated T cells with SPIO particles without poly-L-lysine leads to only a minor amount of SPIO particles present in the cell pellets. Increasing the concentration of PLL from 0 to 1.5 µg/ml at a fixed iron concentration of 25 µg/ml increases the mean iron concentration in the washed cell suspension from an almost undetectable level to 4.2 ± 1.04 µg/ml. Augmenting the iron concentration from 25 µg/ml to 400 µg/ml at a fixed poly-L-lysine concentration of 1 µg/ml results in a 2-3 fold increase in iron uptake up to 10.5 ± 1.13 µg/ml (i.e. approximately 11.7 pg/cell). From these results it can be concluded that labelling of activated rat T cells with 400 µg Fe/ml and 1 µg PLL /ml leads to a high intracellular iron content and minimal free SPIO-PLL aggregates. Quantification of the percentage of labelled cells in this latter condition was performed by means of Easysep. It was demonstrated that approximately 65% of the cells were labelled. The uptake of SPIO particles by myelin reactive T cells at this labelling condition was verified by electron microscopy. Figure 1C demonstrates the intracellular location of the SPIO particles.

Effect of SPIO labelling on cell viability and function

To determine whether the high cellular iron content of cells labelled with 400 µg Fe/ml and 1 µg PLL/ml affects cell function we compared the viability, activation status and cytokine production of these cells with unlabelled cells either directly after labelling or after a post labelling period of 72 hrs. As shown in Figure 2A the viability of the labelled and unlabelled cells is at both time points comparable. The activation status of T cells is reflected by its cell size and the expression of the IL-2 receptor. To examine

whether incubating T cells with Fe-PLL complexes leads to a changed activation status, we compared the expression of the CD25 molecule (i.e. the alpha chain of the IL-2 receptor) of labelled and unlabelled cells. Results demonstrate that in both conditions approximately 90% of the T cells expressed CD25 indicating that the labelling of these cells with SPIO-PLL does not augment or down-regulate the activation status (Figure 2B). Furthermore, the myelin reactive T cells capable of inducing disease are known to have a Th1 cytokine profile. This profile is characterized by the production of IFN-γ and the absence of IL-4 expression. The cytokine profile of the labelled and unlabelled cells demonstrate a high IFN-γ production at day 4 (± 45% IFN-γ+CD3+/CD3+ cells) and day 7 (± 37% IFN-γ+CD3+/CD3+ cells) after restimulation (i.e. directly and 3 days after labelling) whereas no IL-4 producing cells could be detected. The level of IFN-γ production was at both time points comparable for labelled and unlabelled cells (Figure 2C). Together these results indicate that labelling of T cells with 400 µg Fe/ml and 1 µg PLL/ml does not alter the viability, cytokine production or activity of these cells.

Tracking of disease inducing myelin-reactive T cells

Labelled myelin reactive T cells were systemically transferred to naive rats in order to examine the feasibility to track these cells upon infiltration in the spinal cord and the brain of rats and to analyse their distribution pattern. Due to the encephalitogenic capacity of the myelin-reactive T cells animals developed tail and hindlimb paralysis three to four days after transfer. At this time point animals were sacrificed and post mortem imaging of the brain and spinal cord was performed. Figure 3A shows hypo intense areas in the sacral part of the spinal cord, rostral to the cauda

equina, indicative for the presence of the transferred SPIO labelled cells (n=2). Neither in the rostral part of the spinal cord nor in the brain, hypo intense areas were detected.

Tracking of myelin reactive T cells upon transfer in primed rats

Subsequently, we compared the infiltration pattern of myelin reactive T cells transferred in healthy animals to induce disease with the migration pattern of these cells upon transfer in primed rats. Hereto, labelled myelin reactive T cells were i.p. injected in MBP immunised rats at onset of disease (i.e. day 10 p.i.; weight loss, n=2). Three to four days after transfer (i.e. at the occurrence of hindlimb paralysis) post mortem images of the CNS were acquired. Figure 3B shows the presence of hypo intense regions in the lower part of the spinal cord comparable to those observed after transfer of labelled T cells in naive rats. However, hypo intense areas were also present in the brainstem and midbrain. These results demonstrate the feasibility of detecting systemically injected SPIO labelled T cells in the spinal cord as well as in the brain tissue of rats. Furthermore, it reveals that the infiltration pattern of the myelin reactive T cells into the CNS is distinctly different in naive animals and already primed rats. Prussian blue stainings on the caudal part of the spinal cord further indicated the presence of iron oxide labelled cells in this region (Figure 3C). Immunohistochemical stainings using an antibody directed against the CD3 surface marker of T cells confirmed the infiltration of T cells into this CNS region (Figure 3D).

Discussion

In this study, we demonstrate the feasibility to track SPIO labelled myelin reactive T cells into the spinal cord as well as the brain of rats after i.p. injection. To this end we optimized the labelling conditions for rat T cells with SPIO particles and PLL to obtain a high iron load and minimal particle aggregation.

The high proliferation rate of activated T cells combined with their poor phagocytic capacity requires a fine tuned labelling protocol leading to a high iron load of the cells without loss of function. ICP measurements indicated that the amount of iron in the cell pellet is increased at higher PLL concentrations. However, Prussian blue stainings demonstrated that this increase mainly results from an augmented amount of free SPIO-PLL aggregates rather than an improved particle uptake. Upon transfer, the SPIO-PLL aggregates can be taken up by phagocyting cells like blood monocytes and Kupfer cells. A subsequent trafficking of the monocytes to the CNS can lead to hypo intense areas not correlated to the presence of transferred T cells. Our results show that the amount of SPIO-PLL aggregates is highly reduced upon increasing the Fe:PLL ratio, further coinciding with an increased cellular uptake of the iron oxide particles. Labelling of activated rat T cells with a final concentration of 1 µg PLL/ml and 400 µg Fe/ml leads to a high iron load of ± 11 pg Fe/cell and minimal particle aggregates. Using these labelling conditions no effect on the activation status, the cytokine production and the viability of the cells was observed and the labelled cells retained their capacity to induce disease. Anderson et al. and Dodd et al. already demonstrated that incubating CD8+ T cells with SPIO particles without the addition of any TA leads to a cellular uptake of only 0.05 pg Fe/cell even at SPIO concentrations of 2 mg Fe/ml

(7,26). Moreover, since the visualisation experiments of these cells by MRI were restricted to the detection of these cells in a gel matrix, it remains questionable whether these cells are in vivo tractable upon systemic administration. Other research groups already compared different TAs in their ability to increase labelling efficiency and to study their toxicity (8,21). From these studies it became clear that high molecular weight PLL significantly increases the uptake of dextran coated iron oxide particles and is the least toxic TA with adverse affects occurring only above 2 µg/ml, as was confirmed by our study. Berger et al. more specifically indicated a concentration of 1.5 µg PLL/ml and 22.5 µg Fe/ml to be optimal for the labelling of rat T cells using SPIO particles (23). However, since the presence of free SPIO-PLL precipitates at the different SPIO-PLL ratios was not verified, it is not clear whether the measured values result from SPIO particles present within the cells or from free aggregates. Furthermore, the optimal amount of iron to be used was based on viability studies showing a reduced viability of the cells when incubated with iron concentrations > 22,5 µg/ml. In our study, no toxic effects were observed, even not at 400µg Fe/ml. This discrepancy possibly results from a shorter exposure time of the cells to the iron oxide particles in our study (i.e. 24hrs vs 48hrs). Furthermore, a study of Kircher et al. confirms that incubating T cells with CLIO-tat particles containing a similar iron concentration does not lead to any adverse effect (27). Likewise, labelling of other cell types to an even higher iron load was shown not to result in toxicity. Only after incubating cells with > 20 mg/ml Fe a reduced viability was observed (16). Also the cytokine shift of macrophages from a pro-inflammatory to an anti-inflammatory profile after the uptake of (U)SPIO particles, as earlier described by Siglienti et al. (28), did not occur in our labelled T cells. Even more, the labelled T cells retained their

encephalitogenic capacity. Estimating the number of cells being labelled, we found 65% of the cells being retained by a magnet, which is higher as the 60% earlier described by Berger et al. (23).

The feasibility to track labelled myelin reactive T cells into the CNS of rats was investigated after systemic administration of these cells to naive and primed EAE rats. Post mortem images were acquired using a spin echo pulse sequence (p.s.), reducing the amount of susceptibility artefacts and allowing to obtain high quality images (i.e. with high signal to noise ratio and high inplane resolution) of the entire CNS with a length of approximately 10 cm. Due to the encephalitogenic capacity of myelin reactive T cells, naive animals developed EAE upon transfer of these cells. Images acquired at the occurrence of hindlimb paralysis demonstrate that these cells mainly infiltrate in the sacral part of the spinal cord, rostral of the cauda equina, as demonstrated by the presence of clear hypo intense areas. The presence of SPIO particles and infiltrated T cells in this region of the spinal cord was confirmed by a Prussian blue staining and an immunohistochemical staining respectively. The observed infiltration pattern corresponds with earlier findings of Wekerle et al that indicated the presence of myelin reactive T cells in the lower part of the spinal cord based on immunohistochemical stainings using Vβ8.2 directed antibodies (29). Also by means of flow cytometry and GFP transduced myelin reactive T cells, the migration of these cells into the spinal cord upon transfer in naive animals was confirmed (6). However, only the above described method of tracking SPIO labelled myelin reactive T cells with MRI has the potential of a detailed in vivo follow up of the cells throughout the entire CNS. A subsequent research question was whether the infiltration pattern of myelin reactive T cells is different in already diseased EAE rats. Results showed that in the latter case the

transferred cells were widely distributed within the CNS with hypo intense areas being present in the lower part of the spinal cord but also in the brainstem and cerebellum. This points to a different migration and infiltration pattern of myelin reactive T cells upon disease induction or during disease progression. We already demonstrated similarly a gradual shift in the infiltration sites of macrophages in the CNS during disease progression using USPIO particles (30). Earlier studies using BLI could not detect an allocation of MBP reactive T cells in the brain when transferred at disease onset. This disagreement could possibly be explained by a lack of in depth view of BLI which puts a serious restriction on the detection of cells infiltrated in the brain (5).

Conclusions

This study demonstrates the feasibility to track SPIO labelled myelin reactive T cells in the spinal cord as well as the brain of recipient rats upon systemic administration. In this way, we revealed different patterns of autoreactive T cell infiltration into the CNS in either naive rats or already actively immunised EAE rats. Furthermore, we provide data on an optimal labelling protocol towards a high particle uptake, minimal aggregate formation and without any effect on the viability and functioning of the cells. These results can lead to a further implementation of T cell tracking by MRI in EAE, which can be of great importance to investigate the role of different effector and regulatory T cell subsets and to evaluate new therapies.

Acknowledgements

We thank Alice Walter from Laboratoire Guerbet (Paris, France) for kindly providing the SPIO particles (Endorem) and gratefully acknowledge the financial support from the ‘Instituut voor de aanmoediging van Innovatie door Wetenschap en Technologie in Vlaanderen (IWT)’ and the ‘tUL impulsfinanciering’. JJA Hendriks received a postdoctoral fellowship from FWO (Fonds Wetenschappelijk Onderzoek)

Abbreviations

BLI: Bioluminescent Imaging

CNS: Central Nervous System

EAE: Experimental Autoimmune Encephalomyelitis

GFP: Green fluorescent protein

ICP: Inductively coupled plasma mass spectroscopy

MBP: Myelin basic protein

MRI: Magnetic Resonance Imaging

PLL: Poly-L-lysine

SPIO: Small particles of iron oxide

TA: Transfection agent

Figure captions

Figure 1: Determining optimal labelling conditions of rat myelin reactive T cells. Myelin reactive T cells were incubated with variable amounts of SPIO particles and PLL in order to obtain a maximal amount of labelled cells with a high iron load and minimal particle aggregation. A) Prussian blue staining of cells labelled with 25µg Fe/ml and different concentrations of poly-L-lysine (PLL) (first row) and of cells labelled with a fixed amount of PLL i.e. 1 µg/ml and an increasing amount of Fe (second row). B) Quantification of the amount of iron present in the cell pellets for the different labelling conditions as measured by ICP. Data are expressed as mean ± SEM of three experiments. C) Electron microscopic picture of myelin reactive T cells labelled with SPIO particles. The arrow indicates the intracellular location of the particles.

Figure 2: The effect of SPIO-PLL labelling on T cell function. Rat derived myelin reactive T cells were labelled with SPIO particles in combination with PLL (400µg Fe/ml and 1 µg PLL/ml). The viability of the labelled cells was analysed by the MTT assay and compared to unlabelled cells (A). The intensity of the signal obtained from unlabelled cells was set to 1. The effect of labelling on the activation status of the cells was investigated directly after labelling by a flow cytometric measurement of the CD25 expression of CD3+ gated cells (B). The cytokine production of the labelled and unlabelled cells was assessed by analysing the intracellular cytokine production of IFN-γ and IL-4 of TCR+ gated cells directly after labelling and at 72 hrs post labelling. The mean fluorescent intensity (MFI) of the unlabelled cells was set to 1. No significant

amount of IL-4 producing cells could be detected. Data are obtained from three different experiments.

Figure 3: MR imaging of the infiltration of transferred SPIO labelled myelin reactive T cells into the CNS. Myeline-reactive T cells were cultured in vitro, restimulated and labelled with SPIO particles. Subsequently cells were transferred into naive rats (n=2) (A) or in MBP primed rats at the onset of disease (n=2) (B). At the occurrence of hindlimb paralysis, post mortem MRI was performed and coronal images were acquired. Hypointense regions are indicated by white arrows. The presence of SPIO labelled cells in the caudal part of the spinal cord was verified by Prussian blue staining (C). Immunohistochemical stainings of the sacral part of the spinal cord confirm the infiltration of T cells within this CNS region (D).

References

1. Martino G, Hartung HP. Immunopathogenesis of multiple sclerosis: the role of T cells. *Curr.Opin.Neurol.* 1999; **12:** 309-321.

2. Brosnan CF, Raine CS. Mechanisms of immune injury in multiple sclerosis. *Brain Pathology* 1996; **6:** 243-257.

3. Mcfarland HF, Martin R. Multiple sclerosis: a complicated picture of autoimmunity. *Nat.Immunol.* 2007; **8:** 913-919.

4. Ben Nun A, Cohen IR. Experimental autoimmune encephalomyelitis (EAE) mediated by T cell lines: process of selection of lines and characterization of the cells. *J.Immunol.* 1982; **129:** 303-308.

5. Costa GL, Sandora MR, Nakajima A, Nguyen EV, Taylor-Edwards C, Slavin AJ, Contag CH, Fathman CG, Benson JM. Adoptive immunotherapy of experimental autoimmune encephalomyelitis via T cell delivery of the IL-12 p40 subunit. *Journal of Immunology* 2001; **167:** 2379-2387.

6. Flugel A, Berkowicz T, Ritter T, Labeur M, Jenne DE, Li Z, Ellwart JW, Willem M, Lassmann H, Wekerle H. Migratory activity and functional changes of green fluorescent effector cells before and during experimental autoimmune encephalomyelitis. *Immunity.* 2001; **14:** 547-560.

7. Anderson SA, Shukaliak-Quandt J, Jordan EK, Arbab AS, Martin R, McFarland H, Frank JA. Magnetic resonance imaging of labeled T-cells in a mouse model of multiple sclerosis. *Ann.Neurol.* 2004; **55:** 654-659.

8. Arbab AS, Bashaw LA, Miller BR, Jordan EK, Bulte JW, Frank JA. Intracytoplasmic tagging of cells with ferumoxides and transfection agent for cellular magnetic resonance imaging after cell transplantation: methods and techniques. *Transplantation* 2003; **76:** 1123-1130.

9. Beer AJ, Holzapfel K, Neudorfer J, Piontek G, Settles M, Kronig H, Peschel C, Schlegel J, Rummeny EJ, Bernhard H. Visualization of antigen-specific human cytotoxic T lymphocytes labeled with superparamagnetic iron-oxide particles. *Eur.Radiol.* 2008; **18:** 1087-1095.

10. Bulte JW, Ma LD, Magin RL, Kamman RL, Hulstaert CE, Go KG, The TH, de Leij L. Selective MR imaging of labeled human peripheral blood mononuclear cells by liposome mediated incorporation of dextran-magnetite particles. *Magn Reson.Med.* 1993; **29:** 32-37.

11. Bulte JW, Zhang S, van Gelderen P, Herynek V, Jordan EK, Duncan ID, Frank JA. Neurotransplantation of magnetically labeled oligodendrocyte progenitors: magnetic resonance tracking of cell migration and myelination. *Proc.Natl.Acad.Sci.U.S.A* 1999; **96:** 15256-15261.

12. Bulte JW, Arbab AS, Douglas T, Frank JA. Preparation of magnetically labeled cells for cell tracking by magnetic resonance imaging. *Methods Enzymol.* 2004; **386:** 275-299.

13. Bulte JW, Kraitchman DL. Iron oxide MR contrast agents for molecular and cellular imaging. *NMR Biomed.* 2004; **17:** 484-499.

14. Corot C, Petry KG, Trivedi R, Saleh A, Jonkmanns C, Le Bas JF, Blezer E, Rausch M, Brochet B, Foster-Gareau P, Baleriaux D, Gaillard S, Dousset V. Macrophage imaging in central nervous system and in carotid atherosclerotic plaque using ultrasmall superparamagnetic iron oxide in magnetic resonance imaging. *Investigative Radiology* 2004; **39:** 619-625.

15. Daldrup-Link HE, Rudelius M, Oostendorp RA, Settles M, Piontek G, Metz S, Rosenbrock H, Keller U, Heinzmann U, Rummeny EJ, Schlegel J, Link TM. Targeting of hematopoietic progenitor cells with MR contrast agents. *Radiology* 2003; **228:** 760-767.

16. Kustermann E, Himmelreich U, Kandal K, Geelen T, Ketkar A, Wiedermann D, Strecker C, Esser J, Arnhold S, Hoehn M. Efficient stem cell labeling for MRI studies. *Contrast Media & Molecular Imaging* 2008; **3:** 27-37.

17. Pirko I, Ciric B, Johnson AJ, Gamez J, Rodriguez M, Macura S. Magnetic resonance imaging of immune cells in inflammation of central nervous system. *Croatian Medical Journal* 2003; **44:** 463-468.

18. Oude Engberink RD, van der Pol SM, Dopp EA, de Vries HE, Blezer EL. Comparison of SPIO and USPIO for in vitro labeling of human monocytes: MR detection and cell function. *Radiology* 2007; **243:** 467-474.

19. Valable S, Barbier EL, Bernaudin M, Roussel S, Segebarth C, Petit E, Remy C. In vivo MRI tracking of exogenous monocytes/macrophages targeting brain tumors in a rat model of glioma. *Neuroimage.* 2008; **40:** 973-983.

20. Williams JB, Ye Q, Hitchens TK, Kaufman CL, Ho C. MRI detection of macrophages labeled using micrometer-sized iron oxide particles. *J.Magn Reson.Imaging* 2007; **25:** 1210-1218.

21. Arbab AS, Yocum GT, Wilson LB, Parwana A, Jordan EK, Kalish H, Frank JA. Comparison of transfection agents in forming complexes with ferumoxides, cell labeling efficiency, and cellular viability. *Mol.Imaging* 2004; **3:** 24-32.

22. Matuszewski L, Persigehl T, Wall A, Schwindt W, Tombach B, Fobker M, Poremba C, Ebert W, Heindel W, Bremer C. Cell tagging with clinically approved iron oxides: feasibility and effect of lipofection, particle size, and surface coating on labeling efficiency. *Radiology* 2005; **235:** 155-161.

23. Berger C, Rausch M, Schmidt P, Rudin M. Feasibility and limits of magnetically labeling primary cultured rat T cells with ferumoxides coupled with commonly used transfection agents. *Mol.Imaging* 2006; **5:** 93-104.

24. Garden OA, Reynolds PR, Yates J, Larkman DJ, Marelli-Berg FM, Haskard DO, Edwards AD, George AJ. A rapid method for labelling CD4+ T cells with ultrasmall paramagnetic iron oxide nanoparticles for magnetic resonance imaging that preserves proliferative, regulatory and migratory behaviour in vitro. *J.Immunol.Methods* 2006; **314:** 123-133.

25. Montet-Abou K, Montet X, Weissleder R, Josephson L. Cell internalization of magnetic nanoparticles using transfection agents. *Mol.Imaging* 2007; **6:** 1-9.

26. Dodd SJ, Williams M, Suhan JP, imaging, Koretsky AP, Ho C. Detection of single mammalian cells by high-resolution magnetic resonance. *Biophys.J.* 1999; **76:** 103-109.

27. Kircher MF, Allport JR, Graves EE, Love V, Josephson L, Lichtman AH, Weissleder R. In vivo high resolution three-dimensional imaging of antigen-specific cytotoxic T-lymphocyte trafficking to tumors. *Cancer Res.* 2003; **63:** 6838-6846.

28. Siglienti I, Bendszus M, Kleinschnitz C, Stoll G. Cytokine profile of iron-laden macrophages: Implications for cellular magnetic resonance imaging. *Journal of Neuroimmunology* 2006; **173:** 166-173.

29. Lannes-Vieira J, Gehrmann J, Kreutzberg GW, Wekerle H. The inflammatory lesion of T cell line transferred experimental autoimmune encephalomyelitis of the Lewis rat: distinct nature of parenchymal and perivascular infiltrates. *Acta Neuropathol.* 1994; **87:** 435-442.

30. Baeten K, Hendriks JJ, Hellings N, Theunissen E, Vanderlocht J, Ryck LD, Gelan J, Stinissen P, Adriaensens P. Visualisation of the kinetics of macrophage infiltration during experimental autoimmune encephalomyelitis by magnetic resonance imaging. *J.Neuroimmunol.* 2008; **195:** 1-6.

A)

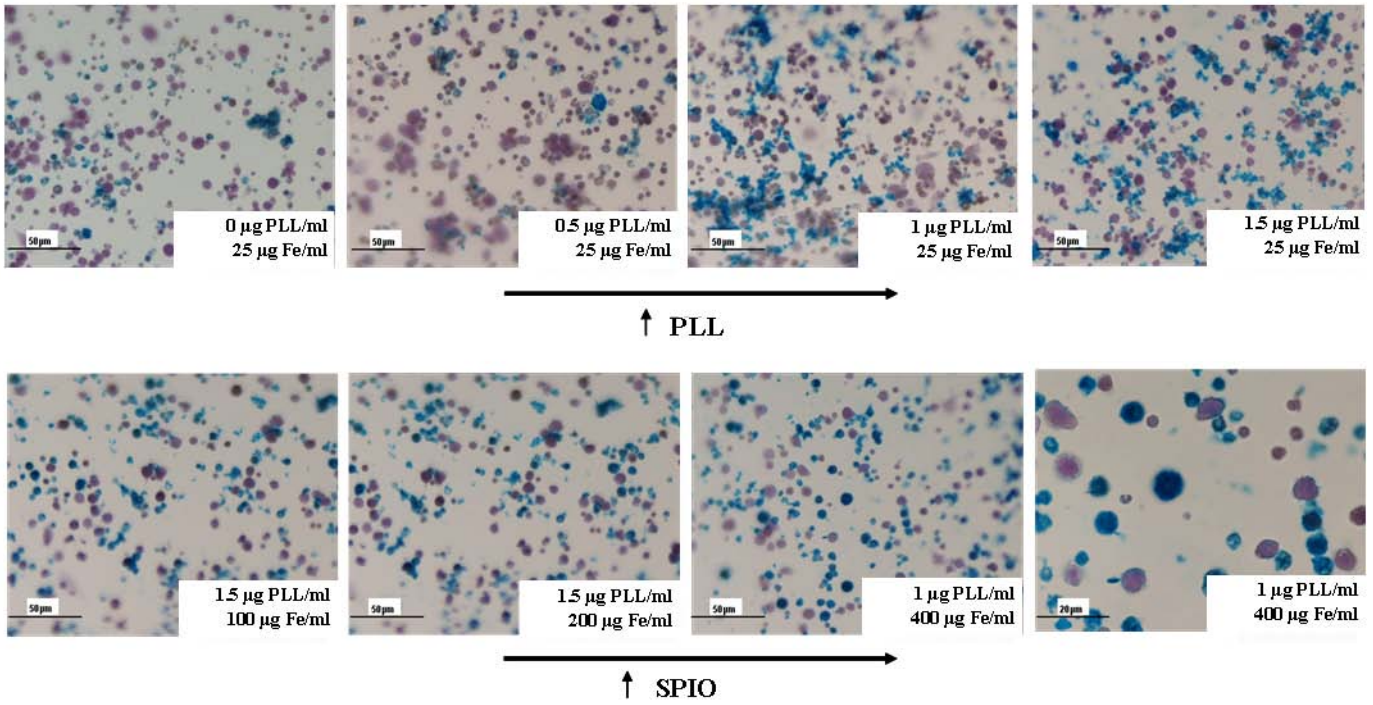
0 µg PLL/ml
25 µg Fe/ml
0.5 µg PLL/ml
25 µg Fe/ml
1 µg PLL/ml
25 µg Fe/ml
1.5 µg PLL/ml
25 µg Fe/ml
PLL
1.5 µg PLL/ml
100 µg Fe/ml
1.5 µg PLL/ml
200 µg Fe/ml
1 µg PLL/ml
400 µg Fe/ml
1 µg PLL/ml
400 µg Fe/ml
SPIO

B)

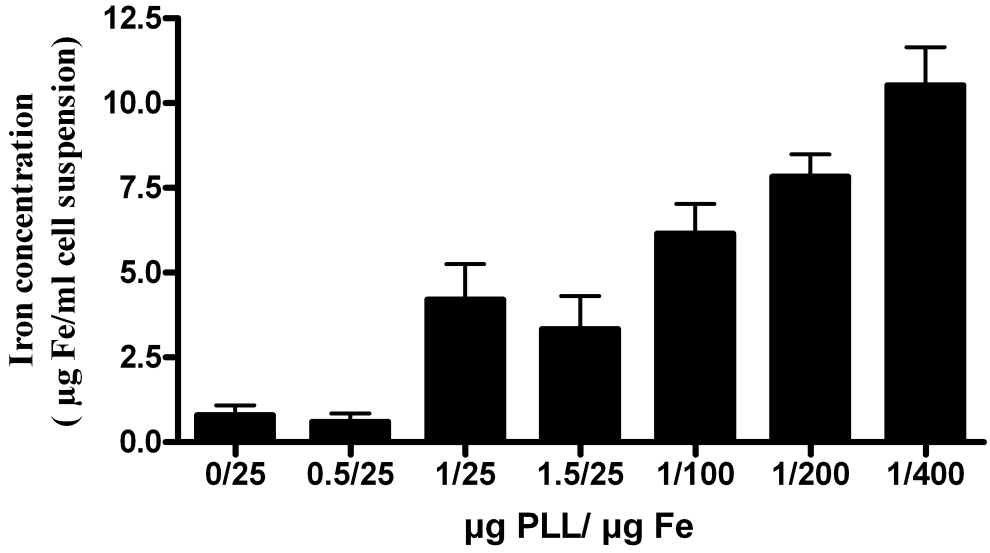

C)

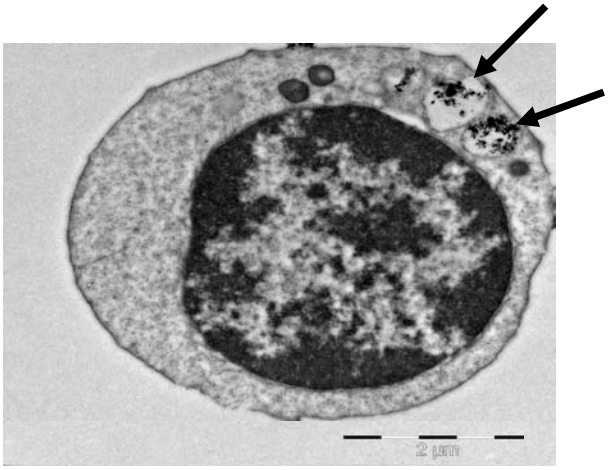

Figure 1: Determining optimal labelling conditions of rat myelin reactive T cells. Myelin reactive T cells were incubated with variable amounts of SPIO particles and PLL in order to obtain a maximal amount of labelled cells with a high iron load and minimal particle aggregation. A) Prussian blue staining of cells labelled with 25µg Fe/ml and different concentrations of poly-L-lysine (PLL) (first row) and of cells labelled with a fixed amount of PLL i.e. 1 µg/ml and an increasing amount of Fe (second row). B) Quantification of the amount of iron present in the cell pellets for the different labelling conditions as measured by ICP. Data are expressed as mean ± SEM of three experiments. C) Electron microscopic picture of myelin reactive T cells labelled with SPIO particles. The arrow indicates the intracellular location of the particles.

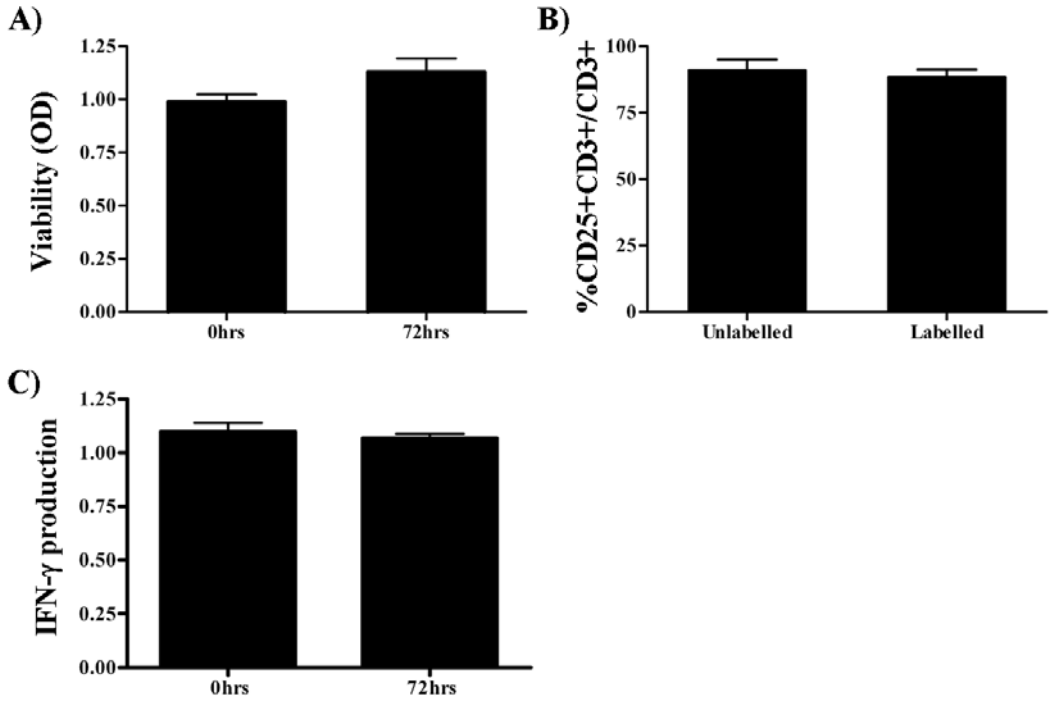

Figure 2: The effect of SPIO-PLL labelling on T cell function. Rat derived myelin reactive T cells were labelled with SPIO particles in combination with PLL (400µg Fe/ml and 1 µg PLL/ml). The viability of the labelled cells was analysed by the MTT assay and compared to unlabelled cells (A). The intensity of the signal obtained from unlabelled cells was set to 1. The effect of labelling on the activation status of the cells was investigated directly after labelling by a flow cytometric measurement of the CD25 expression of CD3+ gated cells (B). The cytokine production of the labelled and unlabelled cells was assessed by analysing the intracellular cytokine production of IFN-γ and IL-4 of TCR+ gated cells directly after labelling and at 72 hrs post labelling. The mean fluorescent intensity (MFI) of the unlabelled cells was set to 1. No significant amount of IL-4 producing cells could be detected. Data are obtained from three different experiments.

A)

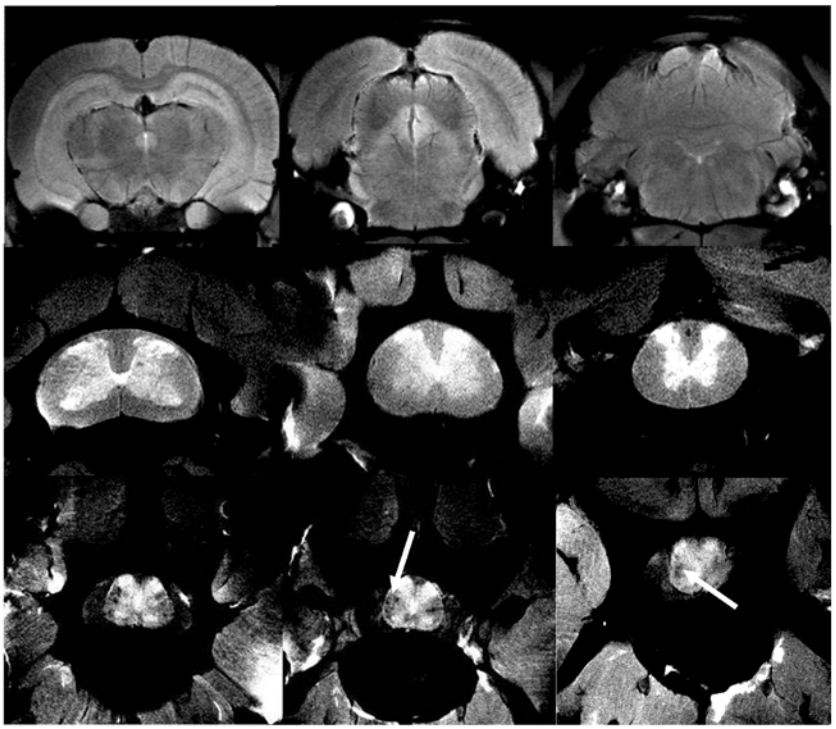

B)

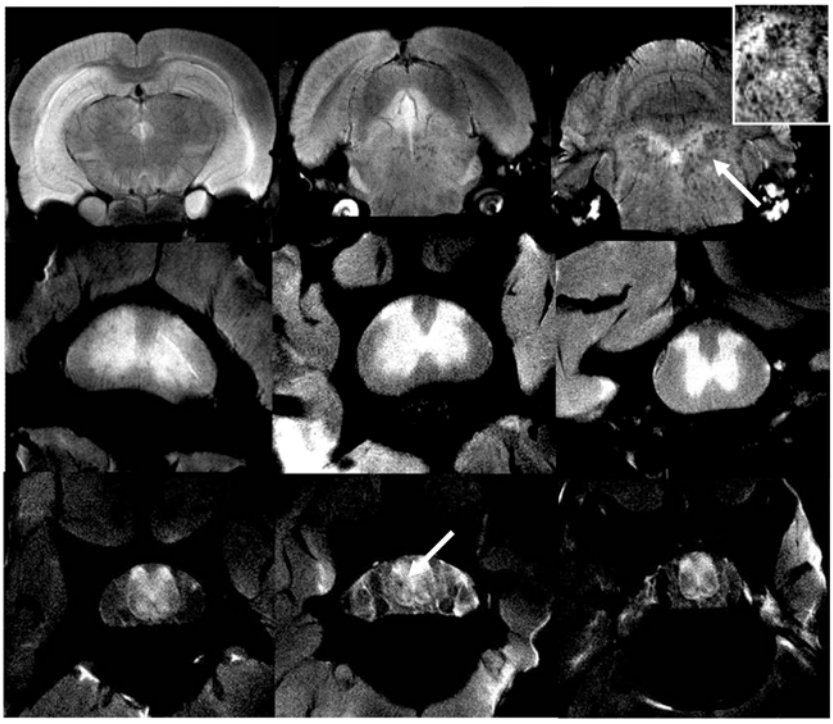

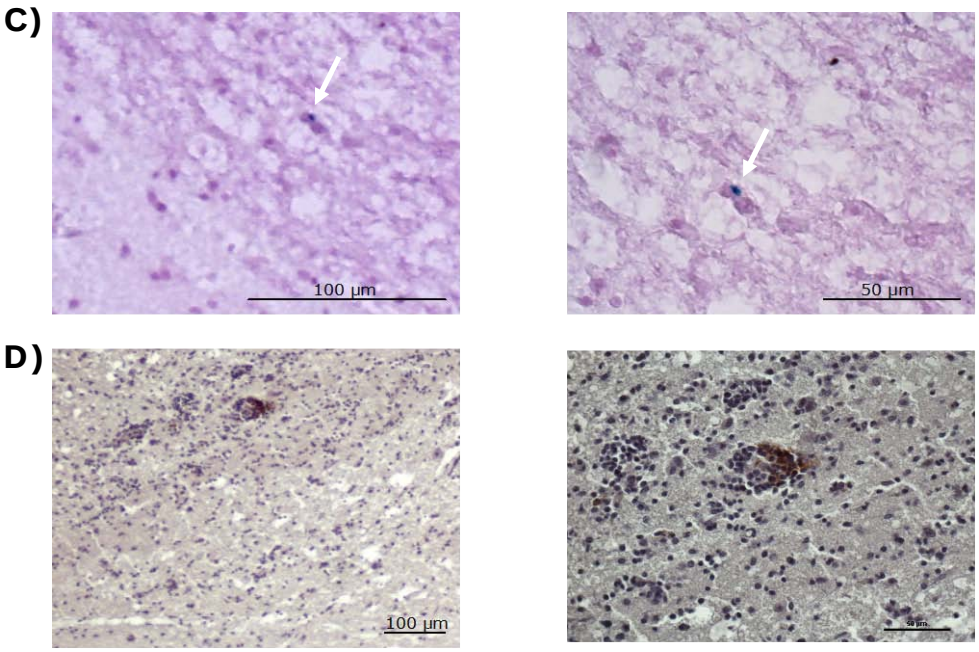

Figure 3: MR imaging of the infiltration of transferred SPIO labelled myelin reactive T cells into the CNS. Myeline-reactive T cells were cultured in vitro, restimulated and labelled with SPIO particles. Subsequently cells were transferred into naive rats (A) or in MBP primed rats at the onset of disease (B). At the occurrence of hindlimb paralysis, post mortem MRI was performed and coronal images were acquired. Hypointense regions are indicated by white arrows. The presence of SPIO labelled cells in the caudal part of the spinal cord was verified by Prussian blue staining (C). Immunohistochemical stainings of the sacral part of the spinal cord confirm the infiltration of T cells within this CNS region (D). Pictures were taken at two different magnifications.